



# Research Journal of Pharmaceutical, Biological and Chemical Sciences

## Hydrothermal Synthesis of MnO<sub>2</sub> Nanoparticles using Teflon Lined Autoclave

M Senthilkumar<sup>a,b</sup>, Balamurugan<sup>b\*</sup>, and BG Jeyaprakash<sup>a,b</sup>

<sup>a</sup>Centre for Nanotechnology & Advanced Biomaterials, <sup>b</sup>School of Electrical & Electronics Engineering, SASTRA University, Tamilnadu, Thanjavur -613 401, India

### ABSTRACT

MnO<sub>2</sub> nanoparticles of different morphology have been synthesized by hydrothermal method using Teflon lined autoclave with cetyl trimethylammonium bromide (CTAB) as capping agent. The structure and morphology of the prepared MnO<sub>2</sub> were studied through X-ray diffraction, Scanning Electron Microscopy and Infrared Spectroscopy at room temperature. The influences of CTAB concentration on the morphology were analysed and reported.

**Keywords:** Teflon lined autoclave, CTAB, hydrothermal, MnO<sub>2</sub>, nanoparticle

*\*Corresponding author*



## INTRODUCTION

In recent years, nanoscale materials have proved to have unique properties than its bulk due to large surface to volume ratio. Among many transition metal oxides, manganese oxide exhibits  $MnO$ ,  $Mn_2O_3$ ,  $Mn_3O_4$ ,  $Mn_5O_8$  and  $MnO_2$  forms. Of which,  $MnO_2$  is the one of the most attractive oxide due to its unique properties. Manganese dioxide ( $MnO_2$ ) is a low band gap, high optical constant semiconductor that exhibits ferroelectric and catalytic properties. It has wide applications, particularly as a reversible-cathode for lithium batteries [1,2], a catalyst for purification of air [3], in removal of CO from hydrogen rich fuel cell [4].

The manganese dioxide has octahedral [ $MnO_6$ ] close packed structure, such that one manganese atom is co-ordinated with six oxygen atom in different ways and forms various crystallographic structure. Thus  $MnO_2$  can exist in  $\alpha$ ,  $\beta$ ,  $\gamma$  and  $\delta$  structural phase, of which,  $\alpha$ - $MnO_2$  has been widely used in lithium based batteries. The properties of  $MnO_2$  strongly depends on microstructure and hence on the processing condition. Different techniques have been reported to obtain  $MnO_2$  nanoparticles, such as solid-state reaction [5], microemulsion [6], sonochemical [7] and hydrothermal method [8]. Surfactant mediated hydrothermal technique is one of the simplest technique for preparing reproducible size and shape of the nanocrystals. Also, the surfactant mediated route exhibit good crystallinity and monodispersity of nanoparticles [9-11]. Huaihao Zhang [12] obtained hollow sphere of  $MnO_2$  nanoparticle through surfactant-assisted co-precipitation method and reported the high specific capacitance of it. Hongju Li et al [13] enumerated the growth of  $\alpha$ - $MnO_2$  nanotube from  $\gamma$ - $MnO_2$  in hydrothermal technique. Nian Tang et al [14] reported the formation of single crystalline  $\alpha$ - $MnO_2$  nanorods in hydrothermal technique through redox reaction between  $MnO_4$  and mixture of  $KMnO_4$  and  $HNO_3$ .

In the present work,  $MnO_2$  nanoparticle of different morphology was prepared using home built teflon lined autoclave unit. The effect of capping agent concentration on the morphology of the particle was studied.

## EXPERIMENTAL

$MnO_2$  nanoparticles were prepared using home built teflon lined autoclave unit. 0.2M of manganese acetate tetrahydrate solution was prepared in deionized water. To this, CTAB of desired concentration is mixed and stirred for 30 minutes. Then 0.4M of sodium hydroxide solution was added under constant stirring. The resultant brown colour solution was then transferred into a Teflon lined stainless steel autoclave and maintained at 300°C for 5 h. The resultant powder was centrifuged at 4000 rpm for 30 minutes and then annealed at 350°C for 3 h. Similarly  $MnO_2$  nanoparticles for different concentration of CTAB were prepared without varying the other parameter and are shown in table 1. The powders were then characterized by powder X-ray diffractometer (XPRT-PRO, PW 3071) using  $Cu-K\alpha$  radiation, (FT-IR) (Spectrum 100, PerkinElmer, USA) and Field emission scanning electron microscope (FESEM JEOL, JSM 6701).

Table 1: Preparation condition for different MnO<sub>2</sub> nanoparticle morphology

Manganese acetate tetrahydrate	Sodium hydroxide	Cetyltrimethyl ammonium bromide	Temperature	Pressure	Volume	Morphology
0.2 M	0.4 M	0.0003 M	300°C	50 bar	30 ml	Nanosphere
0.2 M	0.4 M	0.003 M	300°C	50 bar	30 ml	mixed sphere and rod
0.2 M	0.4 M	0.03 M	300°C	50 bar	30 ml	Nanorod

## RESULT AND DISCUSSIONS

### Structural Analysis

Fig. 1 shows the X-ray diffraction pattern of prepared powders. The XRD pattern exhibited peaks at 18°, 28°, 31°, 36.09°, 38°, 44.41°, 50.7°, 59.88° and 64.70° indicating the formation of tetragonal α-MnO<sub>2</sub>. The peaks were indexed to (200), (310), (101), (211), (301), (411), (521), (002) and (541) planes with respect to JCPDS 44-0141. No impurity peaks such as other phase of manganese oxide and elements were found in the x-ray diffraction pattern, indicating the formation of pure α-MnO<sub>2</sub> particles. The (211) plane was found to have high intense followed by (101) and (310). The presence of different oriented peaks indicates the polycrystalline nature of the particle. Also, all the peaks found to be broadened and indicating the formation of small crystallites. The crystallite size was estimated using Scherer formula.

$$D = \frac{K\lambda}{\beta \cos \theta}$$

Where D is the crystallite size, K is the shape factor, λ the X-ray wavelength, θ the Bragg's angle in radians, and β the full width at half maximum in radians. The crystallite size obtained from the preferentially oriented peak of (211) plane was found to be 30nm.

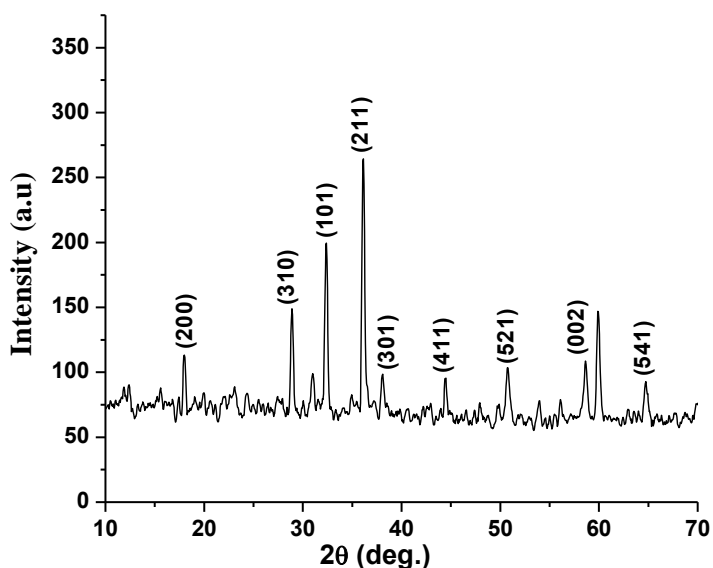


Fig. 1 XRD pattern of α-MnO<sub>2</sub> nanoparticle

### FTIR Studies

Fig. 2 shows the FTIR spectrum of prepared MnO<sub>2</sub> particle. The bands around 3398.36 and 1734.12 cm<sup>-1</sup> corresponds to O-H vibrating mode and is due to physically adsorbed water on MnO<sub>2</sub> crystal from the environment. The bands between 610.54 and 510.65 cm<sup>-1</sup> is the characteristic peak of MnO<sub>6</sub> octahedron of MnO<sub>2</sub> [15-17]. No significant change was observed in the FT-IR spectrum of MnO<sub>2</sub> particles obtained from different CTAB concentration. Also the spectrum does not show other organic groups found in the precursor solution.

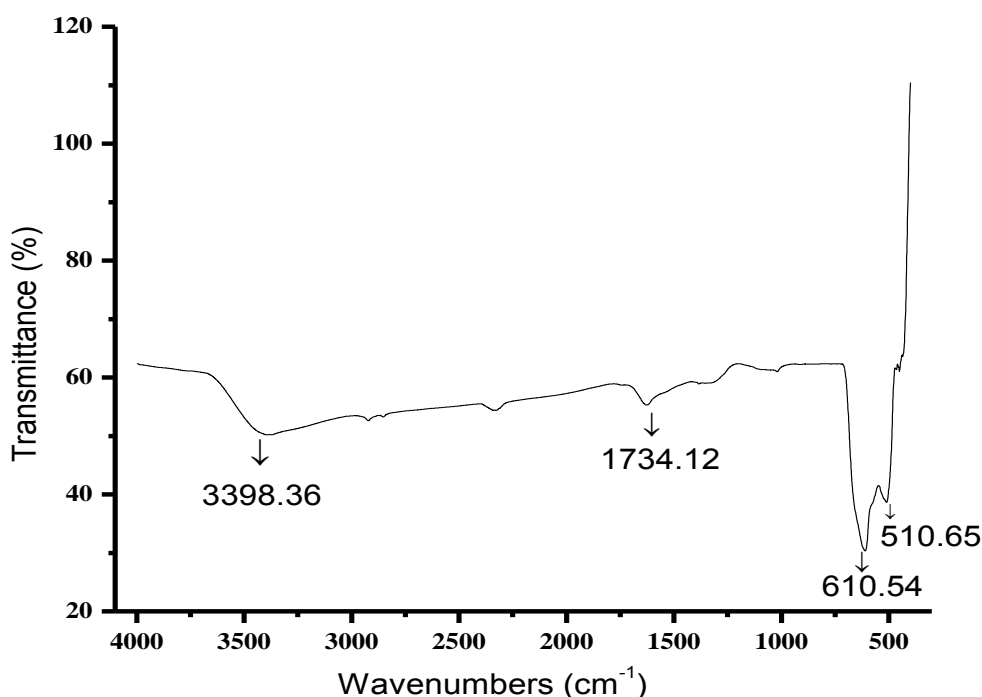
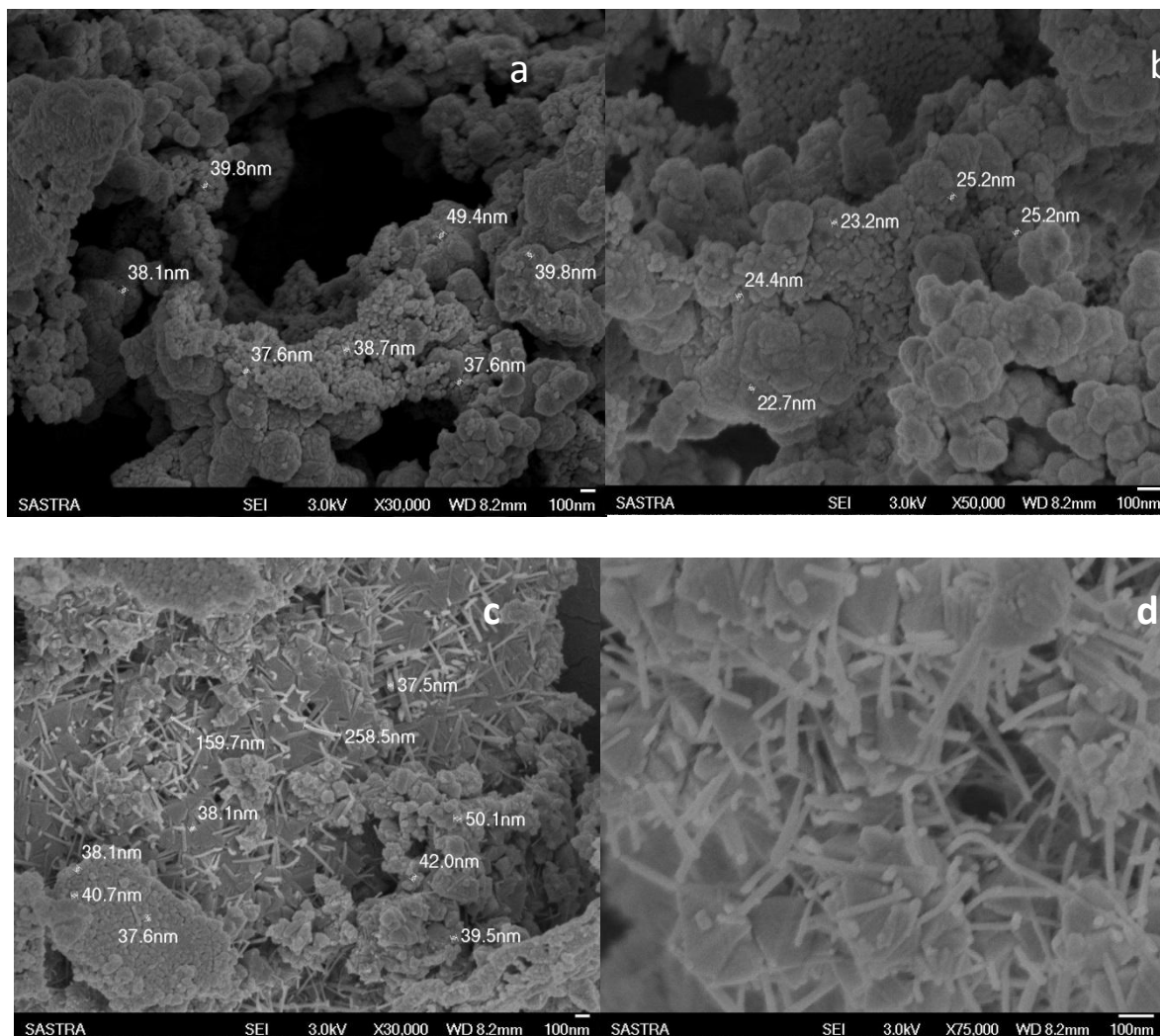


Fig. 2 FTIR spectra of as prepared MnO<sub>2</sub> nanoparticle

### FE-SEM Studies

Fig. 3(a-d) shows the FE-SEM of synthesized MnO<sub>2</sub> powder. Fig. 3(a) indicates the formation of spherical shape particle with size lying between 25 and 40 nm. The observed crystallite sizes also agree with the XRD result. As the concentration of CTAB increases to 0.03M, the morphology changes to mixed sphere and rod (Fig. 3b). Further increase in concentration to 0.3M shows the formation of rods (Fig. 3d). These changes in morphology can be attributed to micelle formation [18] of capping agent. However further studies are required to analyze the growth of MnO<sub>2</sub> nanoparticles in surfactant environment.



**Fig. 3 FESEM of MnO<sub>2</sub> nanoparticles prepared from different CTAB concentration**

### CONCLUSION

MnO<sub>2</sub> nanoparticles have been successfully synthesized by hydrothermal method using teflon lined autoclave with CTAB as capping agent. X-ray diffraction pattern indicates the formation of  $\alpha$ -MnO<sub>2</sub> phase with polycrystalline nature and the preferential orientation was found to be (211) plane. FESEM shows the formation of spherical, mixed spherical-rod and rod like morphology as CTAB concentration increases.

### REFERENCES

- [1] Shao-Horn Y, Hackney SA, Johnson CS, Thackeray MM. J Electrochem Soc 1998;145; 582-589.
- [2] Zoltowski P, Drazic DM, Vorkapic L. J Appl Electrochem 1993; 3: 271-283.
- [3] Jiang B, Liu Y, Wu Z. J Hazard Mater 2009; 146: 1249.
- [4] Zwinkels MFM, Jaras SG, Menon PG, Griffik TA. Catal Rev Sci Eng 1993; 35; 319-358.
- [5] Yuan A, Wang X, Wang Y, Hu J. Electrochimica Acta 2009;54(3):1021-1026.



- [6] Xu C, LiB, Du H, Kang F,ZengY. J Power Sources 2008;180: 664–670.
- [7] Zolfaghari A, Ataherian F, Ghaemi G, Gholami A. Electrochimica Acta 2007;52:2806–2814.
- [8] Yan D, Yan P, Cheng S. Crystal Growth and Design 2009; 9:218–222.
- [9] Zhang Z, Sun H, Shao X, Li D, Yu H, Han H. Adv Mater 2005;17: 42–47.
- [10] Tang Z, Kotov NA, Giersig M. Science 2002;297: 237–240.
- [11] Hou Y,Kondoh H, Ohta T, Gao S. Appl Surf Sci 2005;241:218–222.
- [12] Huaihao Zhang, Yaqiong Wang, Changwei Liu, Haitao Jiang. J Alloys Compd 2012; 517:1– 8.
- [13] Hongju Li, Wen-lou Wang Fangfang Pan, Xiaodong Xin, Qinqin Chang, Xianming Liu. Mater Sci Eng B 2011;176:1054– 1057.
- [14] Nian Tang, XikeTian, Chao Yang, Zhenbang Pi, Qing Han. J Phys Chem Solids 2010;71: 258–262.
- [15] Fang DL, Wu BC, Mao AQ, Yan Y, Zheng CH. J Alloys Compd 2010;507:526.
- [16] Ai ZH, Zhang LZ, Kong FH, Liu H, Xing WT, Qiu JR. Mater Chem Phys 2008; 162-167.
- [17] Ananth MV, Pethkar S, Dakshinamurthi K. J Power Sources 1998;75:278-282.
- [18] Chandrasekaran P, Viruthagiri G, Srinivasan N. J Alloys Compd 2012;540:89-93/